Voltage-dependent Inactivation of Slow Calcium Channels in Intact Twitch Muscle Fibers of the Frog

GABRIEL COTA and ENRICO STEFANI

From the Department of Physiology, Centro de Investigación y Estudios Avanzados del Instituto Politécnico Nacional, México City 07000, México; and the Department of Physiology and Molecular Biophysics, Baylor College of Medicine, Houston, Texas 77030

ABSTRACT Inactivation of slow Ca^{2+} channels was studied in intact twitch skeletal muscle fibers of the frog by using the three-microelectrode voltage-clamp technique. Hypertonic sucrose solutions were used to abolish contraction. The rate constant of decay of the slow Ca^{2+} current (I_{Ca}) remained practically unchanged when the recording solution containing 10 mM Ca^{2+} was replaced by a Ca^{2+}-buffered solution (126 mM Ca-maleate). The rate constant of decay of I_{Ca} monotonically increased with depolarization although the corresponding time integral of I_{Ca} followed a bell-shaped function. The replacement of Ca^{2+} by Ba^{2+} did not result in a slowing of the rate of decay of the inward current nor did it reduce the degree of steady-state inactivation. The voltage dependence of the steady-state inactivation curve was steeper in the presence of Ba^{2+}. In two-pulse experiments with large conditioning depolarizations I_{Ca} inactivation remained unchanged although Ca^{2+} influx during the prepulse greatly decreased. Dantrolene (12 μM) increased mechanical threshold at all pulse durations tested, the effect being more prominent for short pulses. Dantrolene did not significantly modify I_{Ca} decay and the voltage dependence of inactivation. These results indicate that in intact muscle fibers Ca^{2+} channels inactivate in a voltage-dependent manner through a mechanism that does not require Ca^{2+} entry into the cell.

INTRODUCTION

In vertebrate fast-twitch muscle fibers, slowly activated Ca^{2+} channels are mainly located in the membranes of the tubular system (Nicola Siri et al., 1980; Potreau and Raymond, 1980; Almers et al., 1981; Kerr and Sperelakis, 1983). Thus, the decay of the slow Ca^{2+} current (I_{Ca}) during a maintained depolarization could be explained by depletion of tubular Ca^{2+} (Stanfield, 1977; Sánchez and Stefani, 1978; Donaldson and Beam, 1983). In fact, calculations of the amount of Ca^{2+} in the tubular system suggests that during I_{Ca}, depletion may occur (Nicola Siri et al., 1980; Cota et al., 1984). Furthermore, Ca^{2+} depletion explained the decay of I_{Ca} in the cut fiber preparation, under isotonic conditions and with the intracellular medium

Address reprint requests to Dr. Enrico Stefani, Department of Physiology and Molecular Biophysics, Baylor College of Medicine, One Baylor Plaza, Houston, TX 77030.

J. GEN. PHYSIOL. © The Rockefeller University Press · 0022-1295/89/11/0937/15 $2.00 937
Volume 94 November 1989 937–951

equilibrated wth a high concentration of ethyleneglycol-bis(β-aminoethyl ether) *N,N,N',N'*-tetra acetic acid (EGTA) (80 mM) (Almers et al., 1981). On the other hand, the results obtained in intact fibers bathed in hypertonic medium to abolish contraction, suggest that the decay of I_{Ca} is mainly due to inactivation of Ca^{2+} channels. For example, in two-pulse experiments, I_{Ca} during the second pulse can be reduced without any detectable Ca^{2+} entry during the conditioning prepulse (Sánchez and Stefani, 1983; Cota et al., 1984). In agreement with this, the rate of decay of I_{Ca} has a large temperature dependence, and it is not directly related to the peak current amplitude (Cota et al., 1983, 1984).

In view of the differences obtained between intact and cut fibers, in this series of papers we further explored the mechanism of I_{Ca} in both preparations. In this first paper we present additional evidence in intact fibers for voltage-dependent inactivation during I_{Ca} decay. In the following paper, in experiments performed in single cut muscle fibers, we show that the mechanism of I_{Ca} decay depends on the composition of the intracellular solution. We found that intracellular EGTA reduced the voltage dependence of the inactivation process (Francini and Stefani, 1989).

MATERIALS AND METHODS

Electrical Recording

Ca^{2+} channel currents were recorded at 23°C or at 17–18°C in intact fibers from cutaneous pectoris muscle from *Rana montezume* by using the three intracellular microelectrode voltage-clamp method near the fiber end (Adrian et al., 1970). In these experiments we chose the frog *Rana montezume* to be able to compare the inactivation kinetic data with previous work performed in the same frog (Cota et al., 1983, 1984). The techniques and procedures used to calculate membrane currents density are described in detail by Cota et al. (1983). Membrane currents were recorded as the voltage difference $V_2 - V_1$ between the two intracellular voltage microelectrodes. In all current records, linear resistive components were subtracted by analog means. Since Ca^{2+} channels are mainly located in the tubular system (Nicola Siri et al., 1980), fibers with small radii (20–30 μm) were selected to reduce tubular clamp inhomogeneities. Muscle fibers were polarized from their resting potential to −100 mV, which was the holding potential.

Mechanical threshold was optically detected in whole muscle or in bundles of muscle fibers with a two-microelectrode voltage clamp (Chiarandini et al., 1980). The microelectrodes were positioned near the middle of the muscle, one in front of the other, perpendicular to the length of the fiber. Fibers were visualized under a compound microscope with a magnification of 320×, which provided a good resolution of striations. Subthreshold pulses were applied and their strength was increased stepwise until a localized shortening of sarcomeres was detected near the voltage microelectrode, which was in the optical plane. The pulse amplitude was then decreased until the contraction disappeared and this membrane potential was taken as the threshold. The threshold was first determined for a 200-ms pulse and thereafter for shorter pulses.

Solutions

The following recording solutions were used (in millimolar): (*a*) standard solution: 120 tetraethylammonium-methanesulfonate (TEA)-CH_3SO_3, 10 $Ca(CH_3SO_3)_2$ or $Ba(CH_3SO_3)_2$; (*b*) Ca^{2+}-buffered solution: 15 $(TEA)_2$-maleate, 126 Ca-maleate. Maleate provides a convenient Ca^{2+} buffer in the millimolar range. Measurements with calcium-selective electrodes indicate

that Ca^{2+} ion activity is drastically reduced when maleate is substituted for chloride in Tyrode's solution; the ratio of Ca^{2+} ion activity in the presence of maleate to that in normal Tyrode's solution is 0.24–0.32 (Kenyon and Gibbons, 1977). The Ca^{2+} ion activity in the Ca^{2+}-buffered solution was 38 mM. The calculated free Ca^{2+} concentration from the stability constants was 45 mM (Martell and Smith, 1977). When necessary, both recording solutions were made hypertonic by the addition of 350 mM sucrose to abolish contraction. The standard solution contained 2.5 mM K^+ during the recording of resting potentials or Ca^{2+} action potentials and during the determinations of the mechanical threshold.

To further reduce outward K^+ currents muscles were incubated before the experiments at 4°C for 10–14 h in a solution containing (in millimolar): 60 TEA-Cl, 60 CsCl, and 1.8 $CaCl_2$ (Cota et al., 1983). All solutions were buffered to pH 7.00 ± 0.05 with 2 mM imidazole-Cl, and immediately after were filtered through a 0.22 or 0.45 μm millipore filter. Dantrolene sodium (Norwich-Eaton Pharmaceuticals, Norwich, NY) was added to the recording solutions from an aqueous suspension (0.36 mg/ml in 0.1 N NaOH).

Data Analysis

The experimental data were fitted to the proposed function according to the Patternsearch routine (Colquhoun, 1971), which was run in Fortran IV on a microcomputer. The Patternsearch routine minimizes the squared differences between data and the function. Values are given as mean ± SEM, with the number of observations in parentheses.

RESULTS

I_{Ca} Decay Is Not Explained by External Ca^{2+} Depletion

If I_{Ca} decay during a maintained depolarization is due to Ca^{2+} depletion in the transverse tubules, it is expected that buffering the extracellular Ca^{2+} concentration should reduce the rate of I_{Ca} decay (Almers et al., 1981). The experiment shown in Fig. 1 tested this possibility. *A* was obtained at 0 mV from a fiber bathed in the standard recording solution containing 10 mM Ca^{2+} (see Methods); record *B* was obtained at −5 mV from a different fiber in the Ca^{2+}-buffered solution, which contained 126 mM Ca-maleate. The semilog plot of I_{Ca} decay normalized to the peak I_{Ca} for both records is shown in *C* (*open symbols*, standard solution; *filled symbols*, Ca^{2+}-buffered solution). The inward current decays following a similar time course in both cases. This makes it unlikely that Ca^{2+} depletion is the main cause for the decay of I_{Ca}.

In the presence of Ca-maleate, I_{Ca} was detected at ~ −30 mV (effective threshold); for depolarizations to ~ −5 mV the peak I_{Ca} amplitude was −88 ± 17 (5) $\mu A/cm^2$ and the time constant of decay (τ_d) was 0.97 ± 0.12 (5) s. Comparatively, in the standard recording solution the effective theshold was ~ −40 mV (see Fig. 2 *A*, *filled symbols*), and for depolarizations to ~ 0 mV the peak I_{Ca} amplitude was −60 ± 5 (8) $\mu A/cm^2$ and τ_d was 0.91 ± 0.04 s (8).

The positive shift of ~ 10 mV in the effective threshold and the larger peak I_{Ca} amplitude in the Ca^{2+}-buffered solution is consistent with an ionized Ca^{2+} concentration of 30–40 mM (Cota and Stefani, 1984). Because of saturation properties of slow Ca^{2+} channels the fractional increase of peak I_{Ca} amplitude (1.4 to 1.5 times) is smaller than the corresponding increase of ionized tubular Ca^{2+} (3 to 4 times) (Cota

and Stefani, 1984). The larger reserve of Ca^{2+} ions should be sufficient to maintain practically constant the tubular Ca^{2+} concentration during I_{Ca}.

Ca^{2+} Entry Is Not Required for Inactivation of Ca^{2+} Channels

Previous experiments indicated that I_{Ca} can be inactivated by conditioning depolarizations that do not induce detectable Ca^{2+} entry. To further characterize the mechanisms of inactivation of slow Ca^{2+} channels we have analyzed the effects of substitution of Ba^{2+} for Ca^{2+} in the standard recording solution. In addition we have

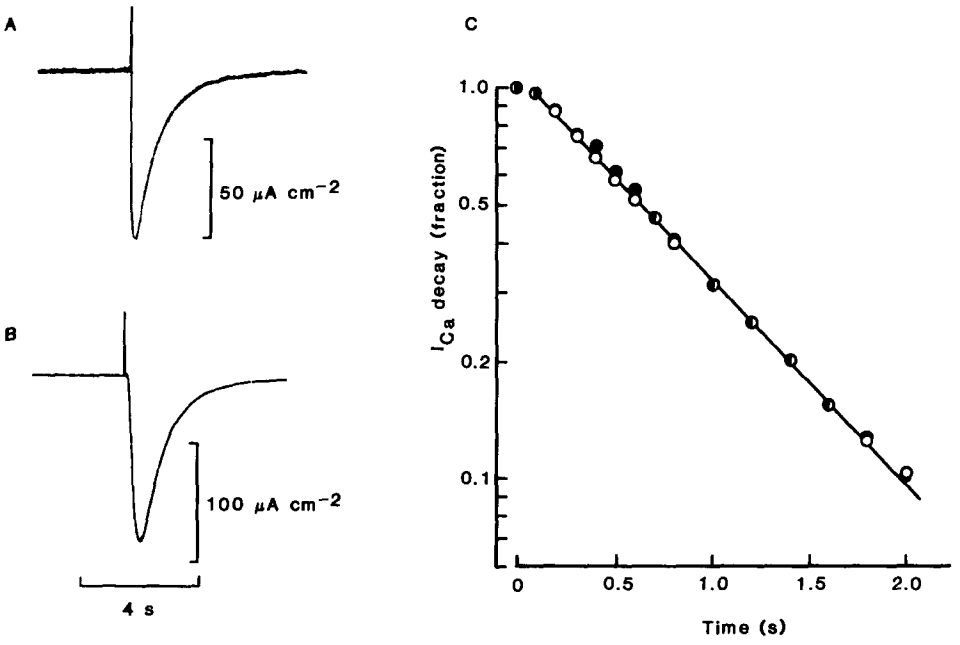

FIGURE 1. Effect of a Ca^{2+}-buffering system on I_{Ca}. I_{Ca} records obtained during maintained depolarizations in two different fibers at 23°C. (*A*) I_{Ca} at 0 mV in the standard recording solution containing 10 mM Ca^{2+}. (*B*) I_{Ca} at −5 mV in the Ca^{2+}-buffered solution containing 126 mM Ca-maleate. (*C*) Semilog plot of I_{Ca} decay in standard recording solution (*open symbols*) and in Ca^{2+}-buffered solution (*filled symbols*). Capacity transients indicate the onset of the depolarizing pulse. For the fiber in *A*: electrical radius, a_e = 28 μm; effective resistance, R_{eff} = 2.50 MΩ, specific membrane resistance, R_m = 6.4 kΩ.cm^2; calibration constant for membrane current, $V_2 - V_1$, 1 mV = 5.15 μA/cm^2. For the fiber in *B*: a_e = 20 μm; R_{eff} = 2.50 MΩ; R_m = 9.0 kΩ.cm^2; $V_2 - V_1$, 1 mV = 2.20 μA/cm^2.

performed two-pulse experiments using large positive prepulses approaching the Ca^{2+} equilibrium potential.

Effects of Ca^{2+} replacement by Ba^{2+}. If Ca^{2+} influx is a contributing factor to slow Ca^{2+} channel inactivation, it is expected that: (*a*) the rate constant of decay of Ba^{2+} currents (I_{Ba}) should be slower than for I_{Ca}, and (*b*) a smaller degree of inactivation of I_{Ba} should be observed in two-pulse experiments (Tillotson, 1979; Brown et al., 1981; Eckert and Tillotson, 1981; Ashcroft and Stanfield, 1983; for reviews see Tsien, 1983; Eckert and Chad, 1984).

Fig. 2 shows the voltage dependence of the peak current amplitude (*A*) and of the rate constant of decay, $1/\tau_d$ (*B*) for I_{Ca} (*filled symbols*) and for I_{Ba} (*open symbols*). The peak current amplitude increases with increasing depolarizations, reaches a maximum value and then decreases as the reversal potential is approached. The maximum current value in the voltage-current relationship is reached ~ 0 mV for I_{Ca} and between −20 and −15 mV for I_{Ba}. In contrast, $1/\tau_d$ for both I_{Ca} and I_{Ba} monotoni-

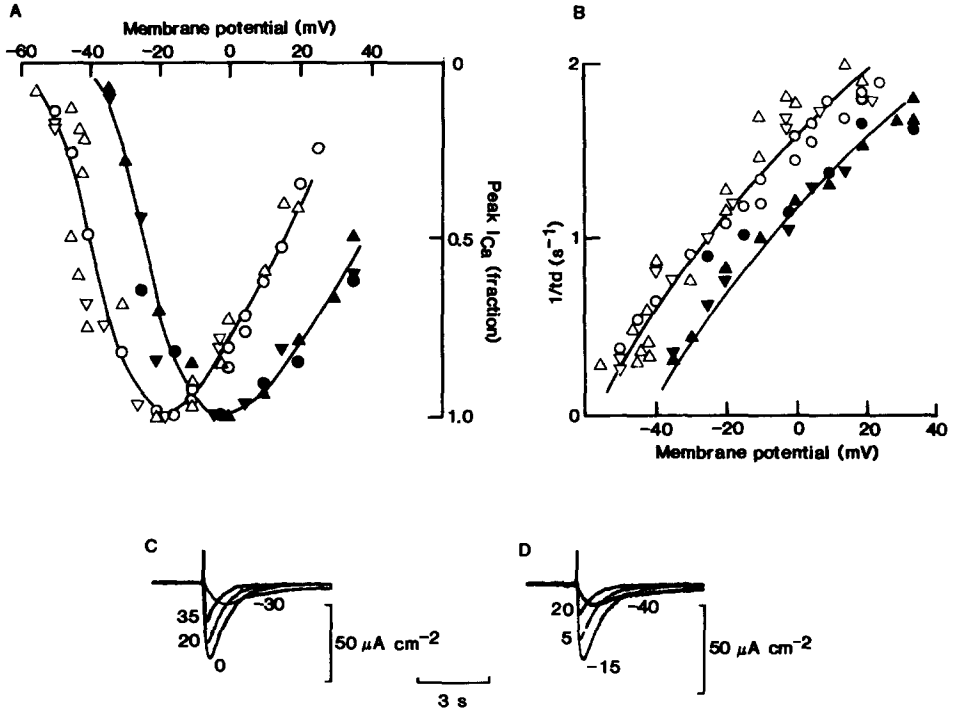

FIGURE 2. Voltage dependence of the rate constant of decay of I_{Ca} and I_{Ba}. (*A*) Normalized peak current amplitudes (*filled symbols*: 10 mM Ca^{2+}, three fibers; *open symbols*: 10 mM Ba^{2+}, three fibers) and *B*, corresponding rate constants of decay as a function of the membrane potential. All data at 23°C. (*C*) I_{Ca} records obtained during depolarizations to different membrane potentials values (indicated by numbers in millivolts) from a fiber bathed in the standard recording solution. (*D*) Inward current records obtained from another fiber at membrane potentials ~ 15 mV more negative than those in *C* after replacement of Ca^{2+} by Ba^{2+} in the recording solution. Capacity transients indicate the ON of the depolarizing pulses. For the fiber in *C*, a_e = 26 μm; R_{eff} = 4.00 MΩ; R_m = 19.2 kΩ.cm²; $V_2 - V_1$, 1 mV = 2.61 μA/cm². For the fiber in *D*, a_e = 26 μm, R_{eff} = 2.88 MΩ; R_m = 10.7 kΩ.cm²; $V_2 - V_1$, 1 mV = 4.31 μA/cm².

cally increases with larger depolarizations. As a conclusion, the faster rate of decay with increasing depolarization (larger $1/\tau_d$) is not related to an increase in peak inward current amplitude. The voltage dependence of both peak current amplitude and $1/\tau_d$ for I_{Ba} is basically similar to that for I_{Ca} but is located 15–20 mV toward more negative membrane potentials. This voltage shift may be explained by surface charge effects (Cota and Stefani, 1984).

The replacement of Ca^{2+} by Ba^{2+} did not significantly modify the $1/\tau_d$ value measured at "comparable" membrane potentials, after correcting for the reported voltage shift. The superimposed traces in Fig. 2 are typical I_{Ca} (*C*) and I_{Ba}(*D*) records from two different fibers, to illustrate the strong similarity of the inward currents recorded at comparable membrane potentials.

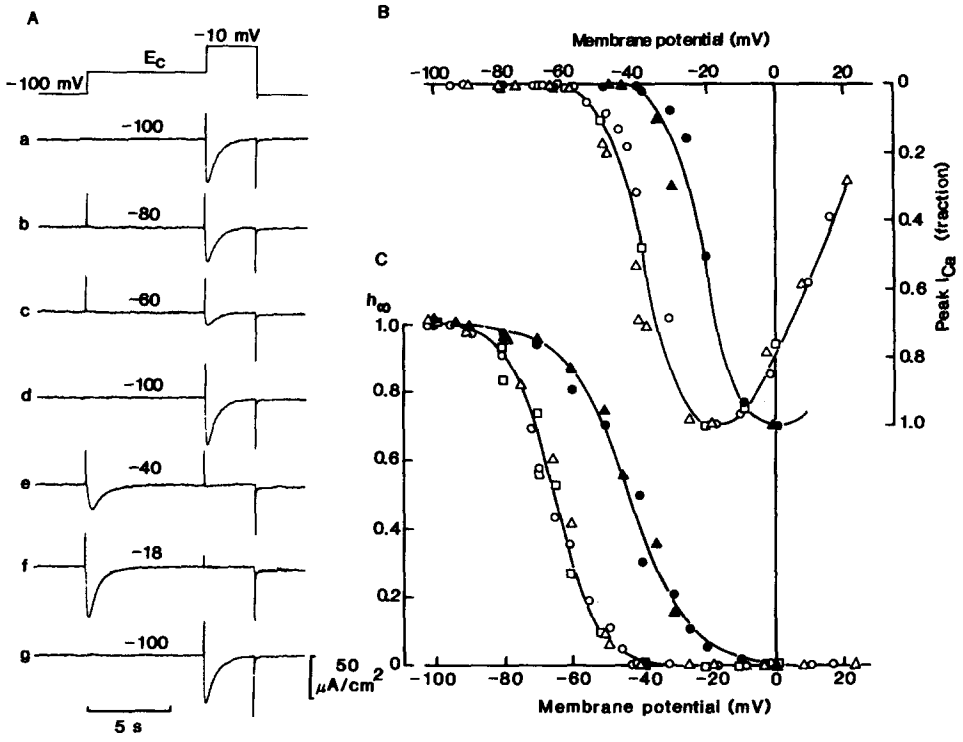

FIGURE 3. Steady-state inactivation of I_{Ca} and I_{Ba}. (*A*) Two-pulse experiment for I_{Ba} at 23°C. The upper trace indicates the pulse protocol: a conditioning 7-s pulse to a membrane potential E_c is followed by a test pulse, in this case, to −10 mV. Records *a–g* are membrane currents that show the effect of increasing the amplitude of the conditioning pulse. Numbers indicate E_C in mV. For this fiber: a_c = 25 μm; R_{eff} = 3.33 MΩ; R_m = 12.7 kΩ.cm²; $V_2 - V_1$, 1 mV = 3.15 μA/cm². (*B* and *C*) Results obtained for I_{Ba} in three fibers (*open symbols*) and for I_{Ca} in two other fibers (*filled symbols*) by using a pulse protocol similar to that in *A*. (*B*) Normalized *I/V* curves during prepulses. (*C*) Normalized peak current amplitude during the test pulse (h_∞) as a function of the membrane potential during the prepulse. In all experiments the duration of prepulses was 7 s and the temperature was 23°C. Test pulses were delivered to 0 mV. Sigmoidal curves in *C* correspond to best nonlinear fit of the experimental points to Eq. 1 (see text).

Fig. 3 *A* shows I_{Ba} records obtained using the two-pulse protocol to investigate the steady-state inactivation curve. Test pulses were delivered to −10 mV and the effect of 7-s conditioning prepulses of various amplitudes on I_{Ba} during the test pulse was studied. Open symbols in Fig. 3, *B* and *C* show the results of this experiment together with those obtained in two other fibers. For comparison, the results

obtained by analyzing I_{Ca} in two other fibers are also shown (*filled symbols*). Fig. 3 *B* shows the voltage dependence of the normalized peak Ca^{2+} or Ba^{2+} current amplitudes during the prepulses, while the plot in Fig. 3 *C* illustrates the fraction of Ca^{2+} channels that are not inactivated as a function of the conditioning potential (steady-state inactivation curve, h_∞). The inactivation parameter was taken as the ratio between either the peak I_{Ca} or I_{Ba} amplitude during the test pulse and that without prepulses. The results with I_{Ca} are similar to those described in Cota et al. (1984). The following observations can be made: (*a*) Ca^{2+} replacement by Ba^{2+} shifts to more negative potentials both the voltage dependence of the current through Ca^{2+} channels, as well as the voltage dependence of h_∞; (*b*) the h_∞ curve is steeper for I_{Ba} than for I_{Ca} indicating that the effect of divalent cation replacement is not a pure voltage shift; (*c*) the fraction of Ca^{2+} channels that can be activated are reduced from 1.00 (at -100 mV) to 0.50 for Ca^{2+} or to 0.30 for Ba^{2+} ions by using prepulses that do not induce detectable inward current; (*d*) depolarizations to -35 mV (with Ba^{2+}) or to 0 mV (with Ca^{2+}) completely inactivate the population of Ca^{2+} channels; (*e*) in the presence of Ba^{2+} the increase of the conditioning depolarization from -20 mV to $\sim +25$ mV, which considerably reduces Ba^{2+} entry into the cell, does not remove Ca^{2+} channel inactivation; (*f*) as for I_{Ca}, the rate constant of decay of I_{Ba} after conditioning prepulses is not dependent on the degree of inactivation; for example, $1/\tau_d$ for I_{Ba} during the test pulse in records *a*, *b*, *c*, and *d* in Fig. 3 *A* is, respectively, (h_∞ in parenthesis): 1.77 (1.00), 1.79 (0.81), 1.75 (0.31) and 1.79 s^{-1} (1.00).

Sigmoidal curves in Fig. 3 *C* were drawn according to the best fit of the experimental points by the relation:

$$h_\infty = 1/\{1 + \exp[(E_m - V_h)/k]\} \quad (1)$$

where E_m is the membrane potential, V_h is the midpoint of the h_∞ curve, and k is related to the steepness of the curve (Hodgkin and Huxley, 1952). For I_{Ca} data, $V_h = -43$ mV and $k = 9.1$ mV, while for I_{Ba} data $V_h = -65$ mV and $k = 6.3$ mV. In a total of nine fibers with I_{Ca} the best fitted parameters were $V_h = -44 \pm 3$ mV and $k = 9.5 \pm 1$ mV, and in six fibers with I_{Ba} $V_h = -65.5 \pm 2$ mV and $k = 6.3 \pm 0.2$ mV.

In conclusion, Ca^{2+} replacement by Ba^{2+} does not reduce the degree of inactivation of Ca^{2+} channels; moreover, in the presence of Ba^{2+} ions the voltage dependence of h_∞ is steeper than with Ca^{2+} ions. Both sets of results in this section indicate that inactivation of Ca^{2+} channels do not require the previous transport of Ca^{2+} or Ba^{2+} into the cell, although the kinetics of inactivation depends on the species of divalent cation that is present in the external medium.

Effect of large positive conditioning prepulses. In the preparations in which Ca^{2+} entry is a prominent factor for inactivation of Ca^{2+} channels the two-pulse protocol using large positive prepulses results in a bell-shaped voltage dependence of the inactivation curve that is roughly parallel to the voltage dependence of Ca^{2+} influx (Tillotson, 1979; Brown et al., 1981; Eckert and Tillotson, 1981; Ashcroft and Stanfield, 1983).

Fig. 4 shows results obtained with I_{Ca} by using 1–2-s prepulses to various membrane potentials, including positive values. The prepulse duration used partially inactivated I_{Ca} and an interval of 0.5 s at -100 mV after the conditioning pulse was

introduced to reduce prepulse activated outward currents at the time of the test pulse. This interval also reestablishes the kinetics of Ca^{2+} channel activation to the resting state (Sánchez and Stefani, 1983). It can be seen in Fig. 4 *A* that by increasing the prepulse depolarization from −30 to 0 mV (records *b–d*) the Ca^{2+} influx during the prepulse also increases, and this effect is associated with a gradually larger degree of I_{Ca} inactivation during the test pulse. However, for depolarizations >0 mV (records *e–g*), the degree of inactivation remains practically unchanged

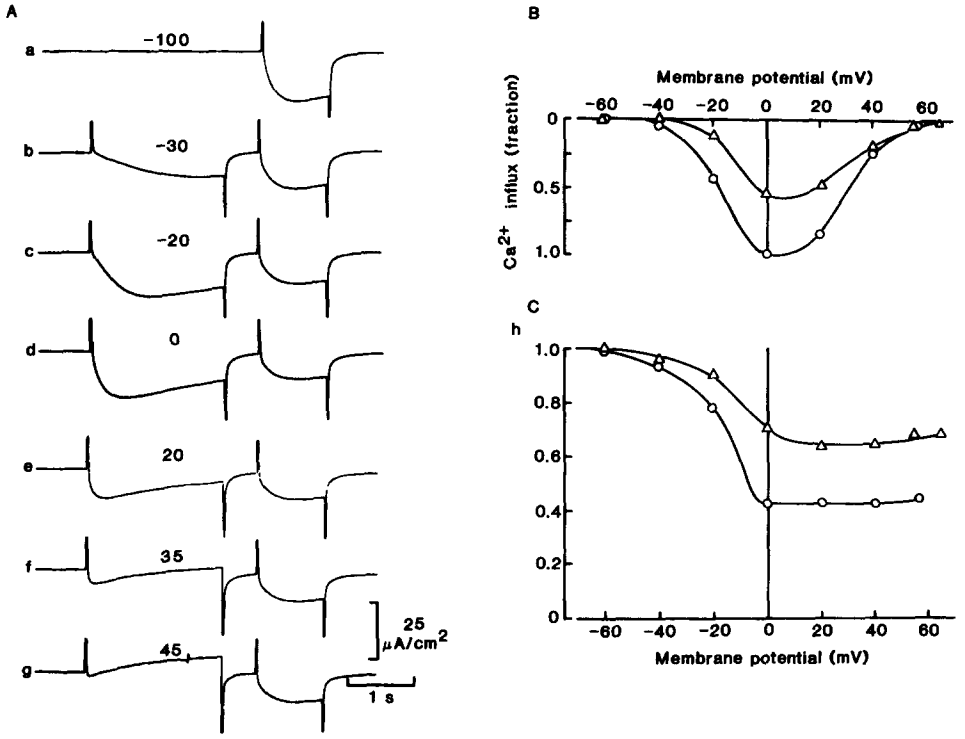

FIGURE 4. Two-pulse experiment for I_{Ca} with positive prepulses. (*A*) Membrane current records from a fiber at 18°C. A 500-ms interval to −100 mV was introduced between the 2-s conditioning prepulse and the test pulse to 0 mV. The numbers indicate the membrane potential during the prepulse. Data of the fiber: a_e = 27 μm; R_{eff} = 6.70 MΩ; R_m = 46.0 kΩ.cm²; $V_2 - V_1$, 1 mV = 2.05 μA/cm². Plots in *B* and *C* show results obtained for I_{Ca} using a two-pulse protocol similar to that in *A* with 1-s prepulses (*triangles*) or 2-s prepulses (*circles*) in a fiber at 17°C. (*B*) Normalized Ca^{2+} influx (inward current-time integral) during prepulses. (*C*) Inactivation parameter *h* (relative peak I_{Ca} amplitude during the test pulse) as a function of the membrane potential during the prepulse.

although I_{Ca} and the Ca^{2+} influx during the prepulse decreases as it approaches the Ca^{2+} equilibrium potential. Figs. 4, *B* and *C* show the results obtained in another fiber by using a protocol similar to that in Fig. 4 *A*. The voltage dependence of Ca^{2+} influx (time integral of I_{Ca}) during the 1- (▽) or 2-s prepulse (○) is plotted in Fig. 4 *B*. Values were normalized with respect to the one for a 2-s prepulse to 0 mV. In Fig. 4 *C* the corresponding voltage dependence of the inactivation parameter *h*

obtained from the peak I_{Ca} during the test pulse to 0 mV is shown. Between 0 and +40 mV there is a drastic reduction of Ca^{2+} entry into the cell but inactivation persists. In conclusion, Ca^{2+} entry into the cell does not contribute significantly to the inactivation of slow Ca^{2+} channels.

Intracellular Ca^{2+} Does Not Inactivate Ca^{2+} Channels

The results presented in the previous section indicate that Ca^{2+} entry is not indispensable for slow Ca^{2+} channel inactivation, however they do not rule out an intracellular Ca^{2+}-dependent inactivation mechanism since Ca^{2+} released from the sarcoplasmic reticulum (SR) into the myoplasm upon depolarization (Ebashi, 1976; Endo 1977; Miledi et al., 1977) can reach an average concentration in the micromolar range (Kovács et al., 1983). In our recording conditions in hypertonic solutions, Ca^{2+} release from the SR upon depolarizing pulses is reduced (Taylor et al., 1979*b*; Parker and Zhu, 1987); thus it should not play an important role for I_{Ca} inactivation. To confirm this, we have further reduced SR Ca^{2+} release with dantrolene sodium since in these conditions SR Ca^{2+} release is abolished and myoplasmic Ca^{2+} transients measured with antipyrylazo III solely reflects Ca^{2+} entry via the slow Ca^{2+} channel (García J., and E. Stefani, unpublished observations).

TABLE I

Membrane Properties of Fibers Bathed in Standard Recording Solution before and after the Addition of 12 μM Dantrolene

	Control	Dantrolene
Resting potential (*mV*)	−92.1 ± 1.3 (7)	−90.5 ± 1.1 (6)
Effective resistance (Ω.10^6)	2.1 ± 0.2 (7)	2.3 ± 0.1 (6)
Electrical radius (*μm*)	25.5 ± 1.0 (6)	29.2 ± 0.06 (14)
Space constant (*mm*)	1.68 ± 0.07 (6)	1.77 ± 0.03 (14)
Internal resistivity (Ω.*cm*)	435 ± 60 (6)	450 ± 20 (14)
Specific membrane resistance (kΩ.cm^2)	9.3 ± 1.0 (6)	9.7 ± 0.4 (14)

Electrical measurements were performed in incubated muscles except the resting potential which was measured in fresh muscles. All data at 23°C.

The inhibitory effect of dantrolene on SR Ca^{2+} release (Taylor et al., 1979*a*) was confirmed by analyzing its effect on the strength-duration curve for the optically detected mechanical threshold. In all experiments, we first examined the strength-duration curve in several fibers bathed in the standard recording solution. Then, the bath solution was exchanged for that containing 12 μM dantrolene and equivalent measurements were carried out 15–20 min after solution replacement. In these experiments, neither the resting potential nor the linear cable properties were significantly modified by dantrolene (Table I).

Dantrolene increased the mechanical threshold at all pulse durations tested. This effect was more pronounced for short pulses, which is in agreement with previous results (Gilly and Constantin, 1974). For example, the mechanical threshold at 18–19°C for 100, 10, and 2-ms pulses was −54 ± 1.0 mV, −43 ± 2.1 mV, and +14 ± 2.3 mV (7), respectively. The corresponding values after the addition of 12 μM dantrolene were −47 ± 1.5 mV, −34 ± 1.7 mV, and +40 ± 3.5 mV (6), respectively.

This observation is consistent with an inhibitory effect of dantrolene on depolarization-induced Ca^{2+} release from SR.

Fig. 5 *A* illustrates I_{Ca} records at various pulse potentials in the presence of 12 μM dantrolene. Fig. 5 *B* compares the voltage dependence of peak I_{Ca} in control experiments (*filled symbols*, six fibers) with that observed in the presence of 12 μM dantrolene (*open symbols*, eight fibers). The current-voltage relationship for peak I_{Ca} is

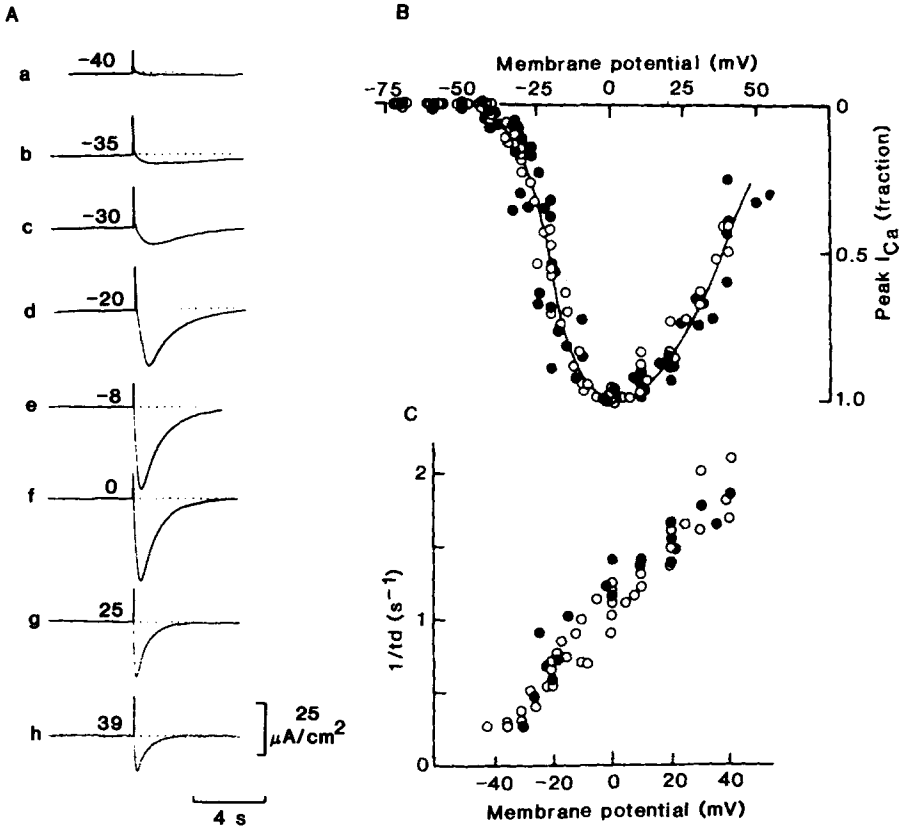

FIGURE 5. Effect of dantrolene sodium on the voltage dependence of peak I_{Ca} and I_{Ca} decay. (*A*) records of I_{Ca} in standard recording solution with dantrolene added (12 μM). Data of the fiber: a_e = 28 μm; R_{eff} = 2.50 MΩ; R_m = 11.1 kΩ.cm²; $V_2 - V_1$, 1 mV = 2.57 μA/cm², 23°C. The plots in *B* and *C* are, respectively, *I/V* curves for the peak value of I_{Ca} and the voltage dependence of $1/\tau_d$ in control experiments (*filled symbols*; six fibers in *B*, three fibers in *C*) and in the presence of 12 μM dantrolene (*open symbols*: seven fibers in *B*, eight fibers in *C*).

about the same in both conditions, which suggests that dantrolene does not modify the voltage dependence of Ca^{2+} channel activation.

Fig. 5 *C* shows the voltage dependence of $1/\tau_d$ rate in control experiments (*filled symbols*, three fibers), and with dantrolene (*open symbols*, seven fibers). Dantrolene does not significantly modify the voltage dependence of I_{Ca} decay.

Fig. 6 *A* shows a two-pulse experiment that was conducted to study the steady-state inactivation curve for I_{Ca} in the presence of dantrolene. Test pulses were deliv-

ered to 0 mV. Prepulses to −50 mV (*b*) or to −60 mV (*c*) did not elicit a detectable inward current, and reduced the size of I_{Ca} induced by the test pulse. Fig. 6 *B* shows the steady-state inactivation curve for I_{Ca} in control experiments (*filled symbols*, three fibers) and in the presence of dantrolene (*open symbols*, three fibers). There are no significant differences between the two sets of experimental points. They were fitted to Eq. 1 with $V_h = -45.5$ mV and $k = 8.3$ mV. These are very similar values to those previously reported (see above). Thus, dantrolene does not affect the voltage dependence of the steady-state fraction of Ca^{2+} channels after conditioning prepulses.

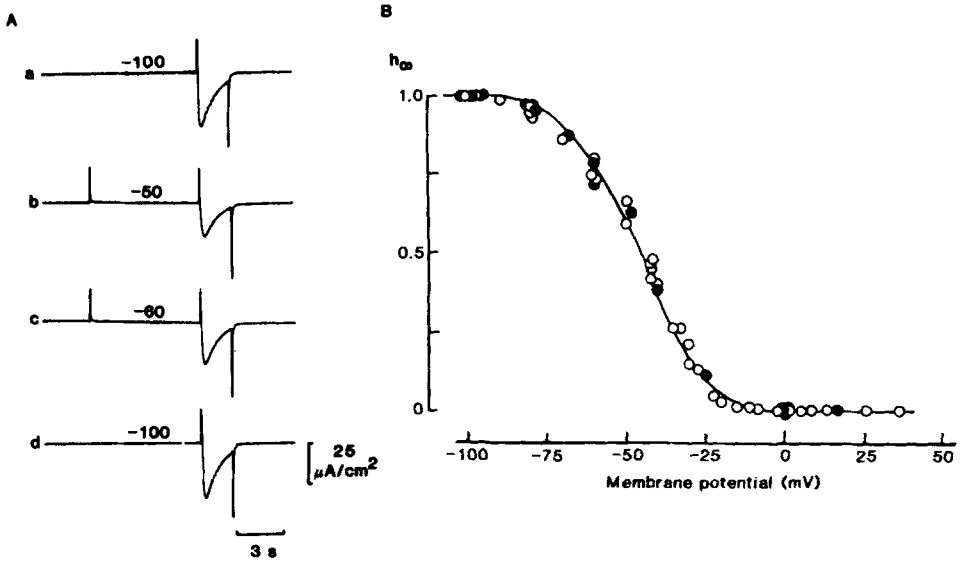

FIGURE 6. Effect of dantrolene sodium on the steady-state inactivation curve for slow Ca^{2+} channels. (*A*) Two-pulse experiment in the presence of 12 μM dantrolene. 2-s test pulse to 0 mV. 7-s prepulses to various potentials (numbers above the records). Data of the fiber: a_e = 31 μm; R_{eff} = 2.00 MΩ; R_m = 8.20 kΩ.cm²; $V_2 - V_1$, 1 mV = 2.90 μA/cm², 23°C. (*B*) Steady-state inactivation curve for I_{Ca}. *Filled symbols*: data from control experiments (three fibers), *open symbols*: data obtained in the presence of 12 μM dantrolene (three fibers). Curve drawn according to Eq. 1 with $V_h = -45.5$ mV and $k = 8.3$ mV.

DISCUSSION

In intact skeletal muscle fibers slow Ca^{2+} channels inactivate through a mechanism that does not require Ca^{2+} accumulation in the myoplasm. This gating process is the principal mechanism for the decay of the current through these channels during maintained depolarization under hypertonic external solutions. The following observations in the present work give strong support to these conclusions, in addition to previous results summarized in the Introduction: (*a*) the rate constant of decay ($1/\tau_d$) of I_{Ca} remains practically unchanged when the standard recording solution is replaced by a Ca^{2+}-buffered solution; (*b*) $1/\tau_d$ of I_{Ca} monotonically increases with depolarization although the corresponding Ca^{2+} influx follows a bell-shaped function; (*c*) the replacement of Ca^{2+} by Ba^{2+} neither results in a slowing of the rate

of decay of the inward current nor reduces the degree of steady-state inactivation; (*f*) the influx of Ca^{2+} ions into the cell does not significantly contribute to an increase in the degree of Ca^{2+} channel inactivation; and (*e*) dantrolene, which reduces Ca^{2+} release from the sarcoplasmic reticulum, does not modify the voltage dependence of Ca^{2+} channel activation and inactivation. In agreement with the voltage-dependent inactivation mechanism, slow Ca^{2+} currents recorded in myoblasts and myoballs in culture had a similar time course of decay as reported here (Caffrey et al., 1987; Toro et al., 1987). Furthermore, recent single Ca^{2+} channel measurements from mammalian skeletal muscle tubular membranes incorporated into bilayers showed a decrease of the open probability during a depolarizing pulse (5 s) from −50 to 0 mV (Fill et al., 1989).

In conclusion, the present results indicate that intratubular Ca^{2+} depletion is not prominent in our experimental conditions. In previous work we considered two possibilities to explain why tubular Ca^{2+} was not reduced during I_{Ca}: (*a*) a large fractional tubular volume, and (*b*) an active transport of Ca^{2+} ions into the tubular lumen from the myoplasm (Cota et al., 1983, 1984). The presence of an inactivation mechanism in the Ca^{2+} channel in our experimental conditions contrasts with the near absence of inactivation reported in cut fibers with high internal EGTA concentrations (80 mM) in this case. Thus high intracellular EGTA impairs the inactivation mechanism (Francini and Stefani, 1989).

An important point that remains open to future investigation is the time course of the current through Ca^{2+} channels and the role of Ca^{2+} released from SR in intact fibers under isotonic solutions. Indirect evidence suggests that in these conditions depletion of intratubular Ca^{2+} may occur during a maintained depolarization (Lorkovic and Rüdel, 1983; Miledi et al., 1983). It is reasonable to assume that in such isotonic conditions there is a smaller fractional volume of the tubular system and that the active Ca^{2+} transport into the tubules is probably not sufficient to avoid tubular Ca^{2+} depletion and so, both processes inactivation and tubular depletion may contribute to determine the decay of the current through Ca^{2+} channels.

Dantrolene increased the threshold for mechanical activation without major changes in I_{Ca}, which indicates that voltage-dependent Ca^{2+} entry is very small and not sufficient to trigger or maintain tension. Similar conclusions were recently obtained in experiments simultaneously measuring I_{Ca} and myoplasmic Ca^{2+} transients (Brum et al., 1987, 1988; Garcia et al., 1989).

In the cut fiber preparation with intracellular K^+ and high EGTA, there is evidence that K currents are activated by Ca^{2+} depletion in the tubular system during I_{Ca} (Palade and Almers, 1985). In their experiments a pharmacological parallelism was found between Ca^{2+} and K^+ currents: K^+ currents of comparable amplitude followed I_{Ca}. In our conditions, K^+ outward currents following I_{Ca} were small, probably reflecting the near absence of Ca^{2+} depletion.

Finally, although Ca^{2+} entry is not necessary for Ca^{2+} channel inactivation, it appears that the voltage dependence of this process is influenced by the divalent cation present in the external medium. In particular, the steady-state inactivation curve tends to be steeper in the presence of Ba^{2+} than in Ca^{2+}. Since Ca^{2+} channel inactivation may be under direct control of the voltage membrane, these observations could be explained by an increase of the magnitude of the effective valence

(z_{eff}) of the voltage sensor of the inactivation gate. Following a two-state model (Keynes and Rojas, 1974; Shlevin, 1979) it may be calculated, from the value of the parameter k in the relation between h and membrane potential, that z_{eff} is ~ 2.8 in the presence of Ca^{2+} and increases to ~ 4.0 after Ca^{2+} replacement by Ba^{2+}. This observation suggests some direct interaction between the divalent cation and the gating mechanism of the Ca^{2+} channel.

This work is dedicated to the memory of Dr. D. J. Chiarandini, to whom the authors and the members of the laboratory are and will be always grateful for his kindness and support we received during his life. The authors are most grateful to Mr. Tomas Estrada for his assistance with the computer programming, to Mr. Eduardo Nieto for building electronic equipment, to Raul Pantoja for clerical assistance and to Alma Ruiz for secretarial work.

This work has been supported by grants PCCBBEU-022519(CONACyT-Mexico) and RO1 AR-38970 (National Institutes of Health) to Dr. E. Stefani.

Original version received 13 December 1988 and accepted version received 26 April 1989.

REFERENCES

Adrian, R. H., W. K, Chandler, and A. L. Hodgkin. 1970. Voltage clamp experiments in striated muscle fibers. *Journal of Physiology*, 208:607–644.

Almers, W., R. Fink, and P. T. Palade. 1981. Calcium depletion in frog muscle tubules: the decline of calcium current under maintained depolarization. *Journal of Physiology*. 312:177–207.

Ashcroft, F. M., and P. R. Stanfield. 1983. Calcium inactivation in skeletal muscle fibers of the stick insect, *Carausius morosus*. *Journal of Physiology* 330:349–372.

Brown, A. M., K. Morimoto, Y. Tsuda, and D. L. Wilson. 1981. Calcium current-dependent and voltage-dependent inactivation of calcium channels in *Helix aspersa*. *Journal of Physiology* 320:193–218.

Brum, G., E. Ríos, and E. Stefani. 1988. Effects of extracellular calcium on calcium movements of excitation-contraction coupling in frog skeletal muscle fibers. *Journal of Physiology* 398:441–473.

Brum, G., E. Stefani, and E. Ríos. 1987. Simultaneous measurements of Ca^{2+} currents and intracellular Ca^{2+} concentrations in single skeletal fibers of the frog. *Canadian Journal of Physiology and Pharmacology*. 65:681–685.

Caffrey, J. M., A. M. Brown, and M. D. Schneider. 1987. Ca currents in BC_3H1 myocytes correspond to those of skeletal muscle T-tubules. *Biophysical Journal*. 51:32*a*. (Abstr.)

Chiarandini, D. J., J. A. Sánchez, and E. Stefani. 1980. Effect of calcium withdrawal on mechanical threshold in skeletal muscle fibers of the frog. *Journal of Physiology*. 303:153–163.

Colquhoun, D. 1971. Lectures on Biostatistics. Clarendon Press, Oxford.

Cota, G., L. Nicola Siri, and E. Stefani. 1983. Calcium channel gating in frog skeletal muscle membrane: effect of temperature. *Journal of Physiology*. 338:395–412.

Cota, G., L. Nicola Siri, and E. Stefani. 1984. Calcium channel inactivation in frog *Rana pipiens* and *Rana montezume* skeletal muscle fibres. *Journal of Physiology*. 354:99–108.

Cota, G., and E. Stefani. 1984. Saturation of calcium channels and surface charge effects in skeletal muscle fibres of the frog. *Journal of Physiology*. 351:135–154.

Donaldson, P. L., and K. G. Beam. 1983. Calcium currents in a fast-twitch skeletal muscle of the rat. *Journal of General Physiology*. 82:449–468.

Ebashi, S. 1976. Excitation-contraction coupling. *Annual Review of Physiology*. 38:293–313.

Eckert, R., and J. E. Chad. 1984. Inactivation of Ca channels. *Progress in Biophysics and Molecular Biology.* 44:215–267.

Eckert, R., and D. Tillotson. 1981. Calcium-mediated inactivation of the calcium conductance in caesium-loaded giant neurones of *Aplysia californica*. *Journal of Physiology.* 314:265–280.

Endo, M. 1977. Calcium release from the sarcoplasmic reticulum. *Physiological Reviews.* 57:71–108.

Fill, M., R. Mejia-Alvarez, S. Hamilton, and E. Stefani. 1989. Voltage inactivation of T-tubule calcium channels incorporated into lipid bilayers. *Biophysical Journal.* 55:297*a*. (Abstr.)

Francini, F., and E. Stefani. 1989. The decay of the slow calcium current in twitch muscle fibers of the frog is influenced by intracellular EGTA. *Journal of General Physiology.* 94:953–969.

Garcia, J., M. Amador, and E. Stefani. 1989. Relationship between myoplasmic calcium transients and calcium currents in frog skeletal muscle. *Journal of General Physiology.* 94:In press.

Gilly, W. F., and L. R. Constantin. 1974. The effect of dantrolene sodium on contractile activation. *Federation Proceedings.* 33:1260.

Hodgkin, A. L., and A. F. Huxley. 1952. The dual effect of membrane potential on sodium conductance in the giant axon of *Loligo*. *Journal of Physiology.* 116:497–506.

Kenyon, J. L., and W. R. Gibbons. 1977. Effect of low-chloride solutions on action potentials of sheep cardiac Purkinje fibers. *Journal of General Physiology.* 70:635–660.

Kerr, L. M., and N. Sperelakis. 1983. Ca^{++}-dependent slow action potentials in normal and dystrophic mouse skeletal muscle. *American Journal of Physiology.* 245:C415–C422.

Keynes, R. D., and E. Rojas. 1974. Kinetics and steady-state properties of the charged system controlling sodium conductance in the squid giant axon. *Journal of Physiology.* 239:393–434.

Kovács, L., E. Ríos, and M. F. Schneider. 1983. Measurement and modification of free calcium transients in frog skeletal muscle fibres by a metallochromic indicator dye. *Journal of Physiology.* 343:161–196.

Lorkovic, H., and R. Rüdel. 1983. Influence of divalent cations on potassium contracture duration in frog muscle fibers. *Pflügers Archiv.* 398:114–119.

Martell, A. E., and R. M. Smith. 1977. Critical Stability Constants. Vol. III. Plenum Publishing Corp., New York. 112–114.

Miledi, R., I. Parker, and G. Schallow. 1977. Measurements of calcium transients in frog muscle by the use of arsenazo III. *Proceedings of the Royal Society, London B.* 198:201–204.

Miledi, R., I. Parker, and P. H. Zhu. 1983. Changes in threshold for calcium transients in frog skeletal muscle fibres owing to calcium depletion in the T-tubules. *Journal of Physiology.* 344:233–241.

Nicola Siri, L., J. A. Sánchez, and E. Stefani. 1980. Effect of glycerol treatment on the calcium current of frog skeletal muscle. *Journal of Physiology.* 305:87–96.

Palade, P. T., and W. Almers. 1985. Slow calcium and potassium currents in frog skeletal muscle: their relationship and pharmacologic properties. *Pflügers Archiv.* 405:91–101.

Parker, I., and P. H. Zhu. 1987. Effects of hypertonic solutions on calcium transients in frog twitch muscle fibres. *Journal of Physiology.* 383:615–627.

Potreau, D., and G. Raymond. 1980. Calcium dependent electrical activity and contraction of voltage-clamped frog single muscle fibres. *Journal of Physiology.* 307:9–22.

Sánchez, J. A., and E. Stefani. 1978. Inward calcium current in twitch muscle fibres of the frog. *Journal of Physiology.* 283:197–209.

Sánchez, J. A., and E. Stefani. 1983. Kinetic properties of calcium channels of twitch muscle fibres of the frog. *Journal of Physiology.* 337:1–17.

Shlevin, H. H. 1979. Effects of external calcium concentration and pH on charge movement in frog skeletal muscle. *Journal of Physiology.* 288:129–158.

Stanfield, P. R. 1977. A calcium dependent inward current in frog skeletal muscle fibers. *Pflügers Archiv.* 368:267–270.

Taylor, S. R., J. R. López, and H. H. Shlevin. 1979*a*. Calcium movements in relation to muscle contraction. *Proceedings of the West Pharmacological Society.* 22:321–326.

Taylor, S. R., H. H. Shlevin, and J. R. López. 1979*b*. Calcium in excitation-contraction coupling of skeletal muscle. *Biochemical Society Transactions.* 7:759–764.

Tillotson, D. 1979. Inactivation of Ca conductance dependent on entry of Ca ions in molluscan neurons. *Proceedings of the National Academy of Sciences.* 76:1497–1500.

Toro, L., M. López, J. Quevedo, and E. Stefani. 1987. Three subtypes of Ca^{++} channels in differentiating mammalian muscle, in culture. *Biophysical Journal.* 51:431*a*. (Abstr.)

Tsien, R. W. 1983. Calcium channels in excitable membranes. *Annual Review of Physiology.* 45:341–358.